N. Gheorghiu,[1,2,*] I. I. Smalyukh,[1] O. D. Lavrentovich,[1] and J. T. Gleeson[2]
[1]Liquid Crystal Institute, Kent State University, Kent, Ohio 44242-0001, USA
[2]Department of Physics, Kent State University, Kent, Ohio 44242-0001, USA
(Received 22 June 2006; published 5 October 2006)

The transition from surface to bulk normal dielectric rolls in a nematic liquid crystal is imaged by fluorescence confocal polarizing microscopy. The three-dimensional director structure and the liquid flow are scanned in both the layer plane and the transverse plane. Two systems of small-scale convective flow are formed, one at each electrode. Strong anchoring makes director oscillations difficult and charges accumulate by the Carr-Helfrich mechanism. The middle region is a structureless convection where the director oscillates with the frequency of the applied voltage. The small-scale flow eventually fills the cell from one electrode to the other as one system of thin and elongated rolls. The true dielectric mode is not a director pattern, rather a surface flow instability.

DOI: 10.1103/PhysRevE.74.041702 PACS number(s): 61.30.−v, 47.54.−r, 47.20.−k, 33.50.−j

Liquid crystals [1,2] (LCs) continue to be very attractive both for their display applications [3–6] and for studying pattern formation on a convenient scale [7–11]. In particular, electrohydrodynamic instability (EHI) in nematic liquid crystals (NLCs) provides many interesting situations for studying pattern formation in an anisotropic dissipative system [12,13]. The standard configuration for EHI is when a NLC thin film is confined between two parallel conducting glass plates where it has a planar (homogeneous) alignment. The rotational symmetry of the NLC director is broken in the layer plane and, therefore, the system is anisotropic in this plane. When an alternating voltage is applied across the layer plane, the dynamics of the director field, the fluid flow, and the electric charge field exhibit two different modes [13–15]. In the low-frequency or conductive mode, the director and the fluid flow are stationary, while the charge follows the applied alternating current (ac) drive. While increasing the threshold voltage is of the order of 10 ^{2}–10^3, and therefore boundary conditions are not important. Above the cutoff frequency f_c, there is the so-called dielectric mode. TheNLCs, one would like to find where and on what scale convection first starts. These are still challenging questions, although they have been specifically raised a few decades ago [21,22]. Experiments in which the direction of the applied electric field was either parallel [23–26] or transverse [27,28] to the direction of optical observation revealed the dielectric instability localized at the cell electrodes. The observation of the true dielectric mode can be difficult, because it can be easily confused with the isotropic mode of EHI [15] that can be observed in any ordinary fluid. In thick cells, the inertial terms in the Navier-Stokes equations play an important role.

≈ 1 Hz [29]). During this time, the dielectric torque applies a shear rate on the director field [30] at the same frequency as that of the driving voltage. The isotropic mode is insignificant in thin samples, at low frequencies, and for a high-viscosity material [15]:

$$1/\tau_D \ll \omega \ll \pi^2 \alpha_{av}/\rho_{av} d^2 \quad (1)$$

where $\tau_D = \epsilon_0 \epsilon_\parallel / \sigma_\parallel$ is the dielectric relaxation time, $\omega = 2\pi f$, with f the frequency of the ac drive, α_{av} is the average Leslie

coefficient, whose value can be increased by lowering the temperature, ρ_{av} is the average density, and d is the layer thickness. Indirect experimental evidence [31], using a twisted cell geometry in a laser scattering setup [32], found that in the dielectric mode the fluid flow has a three-layer structure, consisting of two layers of antiparallel vortices located near the electrodes, and structureless convection in the cell middle. This kind of structure for the fluid flow was actually obtained from calculations and predicted to be the precursor of turbulence [33]. There is no surprising coincidence here, since it is the stabilizing dielectric torque (for a material with $\epsilon_a < 0$) that suppresses the convective instability at high voltages in the conductive mode or at high frequencies in the dielectric mode. Despite all this, a full understanding of the dielectric mode is still missing. The most discussed issue is, still, whether the patterns are bulk instability or rather surface rolls located at the electrodes. Polarizing microscopy in the transverse observation [26] showed small-scale stationary flow in the form of growing plumes located near electrodes, and breakdown of convection in the cell middle. Test particles were observed to execute an oscillatory motion directed along the applied field, indicating the presence of small vortices [21,29] and a nonuniform field distribution near the electrodes [34].

The high-frequency dielectric mode of the EHI exhibits effects not described by the standard model (SM) [35]. The isotropic flow instability represents a challenge for the SM since it can be obtained in any ordinary (isotropic) liquid. The instability is driven by inverted charge gradients in thin Debye layers near the electrodes [15] and this is something

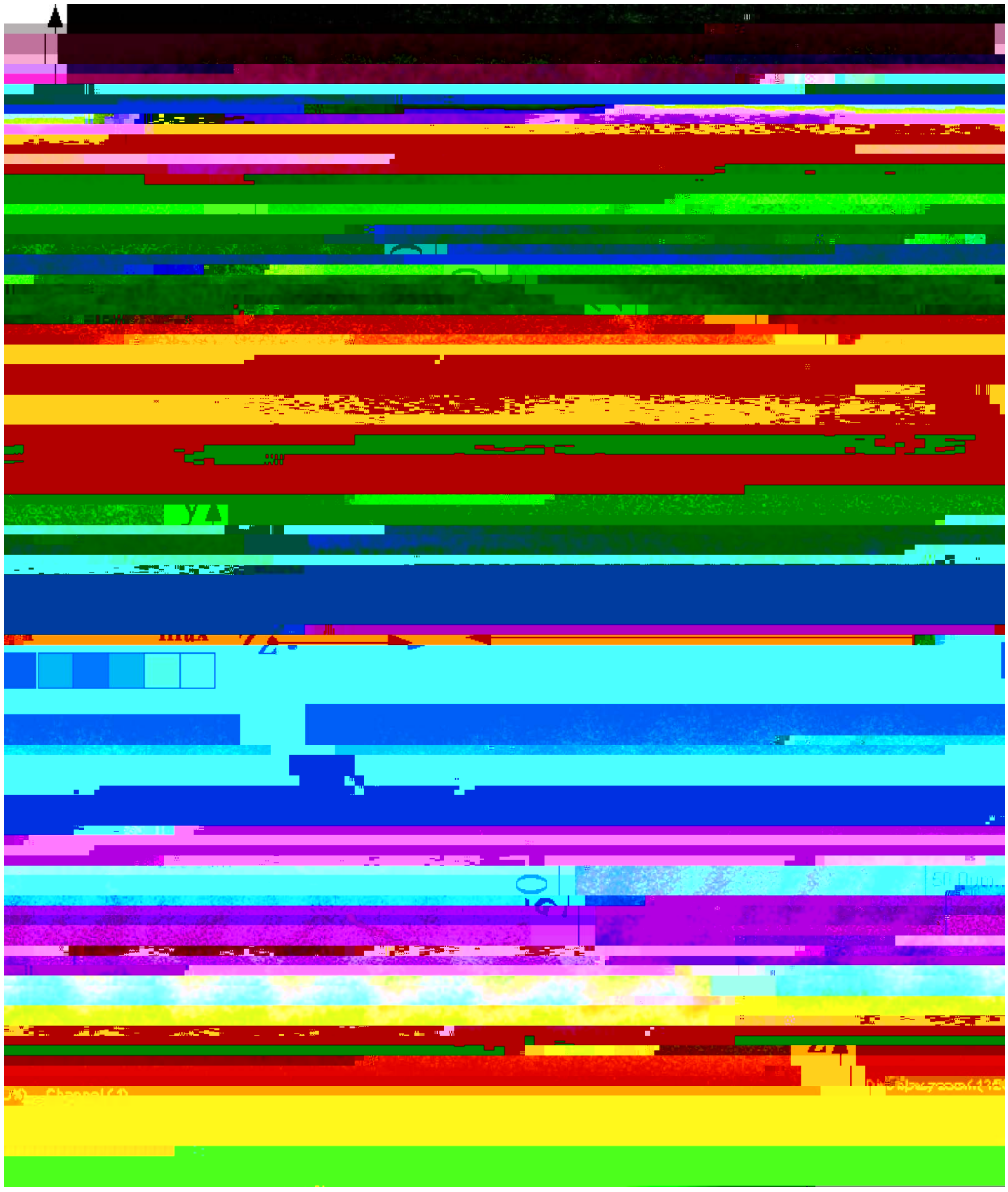

FIG. 3. (Color online) FCPM of normal rolls. At a frequency $\nu = 10$ Hz, the applied square ac voltage is $V = 8.10$ V. The threshold voltage was $V_c = 7.98$ V.

light. The dye concentration was chosen such that the fluorescent signal would be strong enough to give sufficient information about localization of convective patterns. On the other hand, the level of doping was chosen well below the solubility limit. Increasing the concentration of the fluorophore molecules will increase the fluorescence signal as long as these molecules do not get too close together. When fluorophore molecules are within a few nanometers of each other they begin to quench each other. Proximity-induced energy or charge transfer between fluorophores multiplies the efficiency of the quenchers [42]. The fluorescence lifetime for BTBP dye is $\tau_f = 3.7-3.9$ ns, smaller than the characteristic time of rotational diffusion $\tau_d \sim 10$ ns [37,43]; therefore the dye orientation is not changed during the absorption-emission sequence. BTBP molecules absorb laser light and then relax to the ground state by fluorescence or by nonradi-

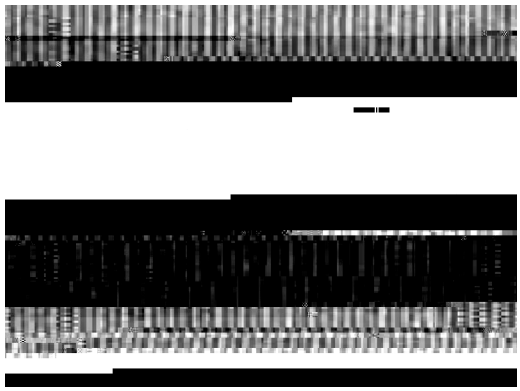

FIG. 4. Shadowgraph image of normal dielectric rolls. The image size is 177×133 μm^2.

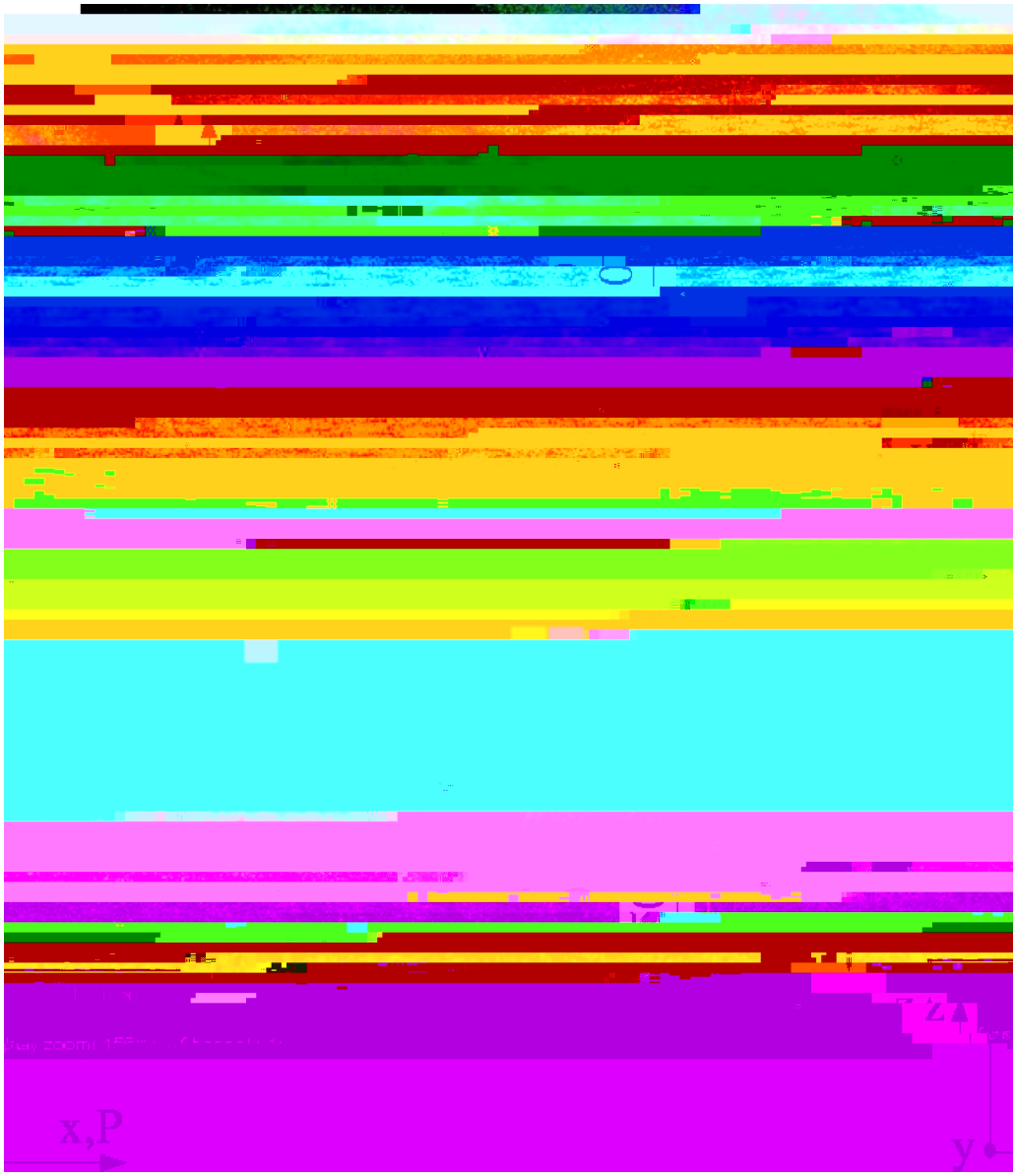

FIG. 5. (Color online) FCM of two layers of normal dielectric rolls, located one at each electrode. The applied square ac voltage is $V = 28.9$ V at a frequency $\nu = 60$ Hz. The threshold voltage was $V_c = 28.8$ V.

ative internal conversion. The Stokes shift is given by the difference between the wavelength of the fluorescence light and that of the absorbed light. Since the spectral absorption dipole is along the long axis of the BTBP molecule, there is a maximum absorption when the polarization of light is along the same direction. The intensity of the fluorescence signal when the input light is polarized has the dependence $I \sim \cos^4 \beta$, where β is the angle between the direction of light polarization and the director [36,37,44].

The NLC was confined between two indium tin oxide–coated glass substrates: one 1.1 mm thick, and the other only 0.17 mm thick [45]. Homogeneous alignment (along) for the nematic director was achieved by rubbing the polyimide (PI2555) coating of the glass substrates. The two substrates were assembled with their coating alignment antiparallel to each other. The obtained LC cell was placed on the microscope stage with the thin substrate at the top, such that the laser beam would enter first through this substrate, thus giving optimal resolution for the FCPM images. The gap d between the two glass electrodes was chosen large enough for a separation of dielectric rolls to be seen. At the same time, the value of d was limited by the axial defocusing of the two propagating modes (extraordinary and ordinary) of the laser beam in the anisotropic LC [36,37]:

$$\Delta = (\Delta / _{av}) \tag{2}$$

where is a dimensionless coefficient of the order of unity that depends on the geometry of light propagation, $\Delta =$ $-$ is the birefringence of the anisotropic medium, with and the indices of refraction for the extraordinary and the ordinary ray, respectively, and is the depth of scanning. The average index of refraction $_{av}$ is evaluated as

$$\varepsilon_{av} = \frac{2\varepsilon_{\perp} + \varepsilon_{\parallel}}{3}. \quad (3)$$

The lower the birefringence $\Delta\varepsilon$ of the material and (or) the smaller the depth d of scanning, the better the resolution of the FCPM image. For Mischung 5, the birefringence $\Delta\varepsilon$ drops from 0.147 at 15.5 °C to 0.082 at 68.5 °C [40]. The advantage for the in-depth resolution of using the small birefringence of the material at high temperatures was not taken. First, the stabilization of NDRs was possible only at low temperatures, where the viscosities were higher, although the birefringence was also larger. Second, and most important, was the necessity to lower the threshold for the dielectric mode below the threshold for the isotropic mode. The results presented here were obtained at $T = 15.0$ °C, for

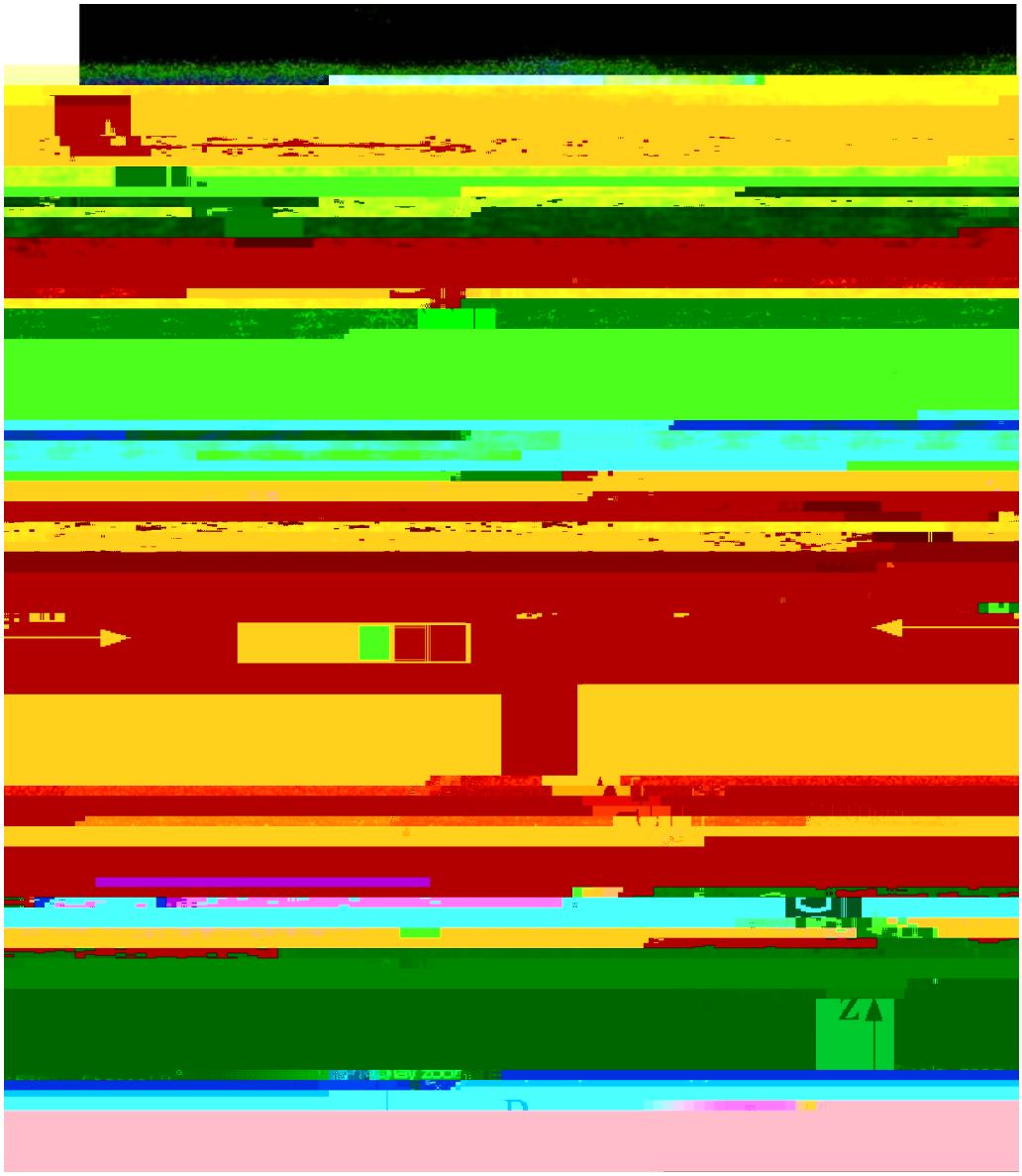

FIG. 7. (Color online) FCM of one layer of dielectric rolls. The applied square ac voltage is $V=33.1$ V at a frequency $=60$ Hz.

unperturbed director. The available region for light focusing is larger at the bottom substrate (toward the laser light source) than at the upper substrate. The counter effect is light absorbtion and increased defocusing near the bottom electrode. These two effects make the image asymmetric along the axis. Above the threshold for the dielectric mode, the shadowgraph observation shows the NDR pattern very similar to Williams-Kapustin domains, except for the very low contrast and also the very small wavelength not scaling with the cell gap (Fig. 4). FCM scans revealed convective layers located one at each electrode (Fig. 5). The scan shows that the NDR instability develops first at the electrodes as small-scale flow. Strong anchoring makes director oscillations difficult and charges accumulate by the CH mechanism. In the cell middle, about 5–8 μm from the 31 μm cell gap, the intensity of the fluorescence mapping shows a minimum. That is nothing else but a reflection of the fast oscillation of the director with the frequency of the driven voltage and, at the same time, an indication of the absence of any flow pattern. Since FCM and not FCPM was used, regions with higher fluorescence intensity must have higher dye concentration. We expect these regions to be also characterized by slower dynamics. Therefore, the lower fluorescence intensity in the cell middle should indicate a fast dynamics of the LC director. Moreover, if the cell middle were convection-free, we would see higher fluorescence intensity with FCPM, but this did not happen. This situation is schematically described in Fig. 6. As Fig. 5 shows, nonuniform fluid flow is also manifested in the layer plane by the coexistence of two-layer and one-layer convection, which was attributed to the high sensitivity of the EHI to the local heating given by the laser beam. The roll width is about 2–3 μm, while its depth is about 10–13 μm. This gives a ratio of roll width to cell gap ranging from 10 to 16. At finite distance from the threshold, the convection filled the cell in only one layer of elongated rolls (Fig. 7), as the Orsay Liquid Crystal Group predicted

[48]. Increasing even more the applied voltage, the chevron pattern set in. While the in-plane transmission scan revealed the defect-mediated chevron pattern, both the in-plane and in-depth FCPM scans showed the absence of any director or flow pattern. The chevron pattern is clearly the optical image of the director fast oscillation and, therefore, cannot be detected by the FCPM scans.

.

As first observed for chevrons [25,28], our observations found that NDRs too are flow patterns and not the result of bending oscillation of the director. We observed this in a not very thick cell, while previously reported optical observations used thick cells too [26]. The SM can explain the transition from bulk to surface NDRs for the lower limit of the

L , d C . a Ma • a (Springer-Verlag, New York, 1994).
[16] E. F. Carr, Mol. Cryst. Liq. Cryst. , 253 (1969).
[17] W. Helfrich, J. Chem. Phys. **1**, 4092 (1969).
[18] S. Rasenat, G. Hartung, B. L. Winkler, and I. Rehberg, Exp. Fluids , 412 (1989).
[19] R. Williams, J. Chem. Phys. **3** , 384 (1963).
[20] A. P. Kapustin and L. K. Vistin, Kristallografiya **10**, 118 (1965).
[21] L. M. Blinov, A. N. Trufanov, V. G. Chigrinov, and M. I. Barnik, Mol. Cryst. Liq. Cryst. **4**, 1 (1981).
[22] A. N. Trufanov, L. M. Blinov, and M. I. Barnik, Zh. Eksp. Teor. Fiz. , 622 (1980).
[23] R. Chang, Mol. Cryst. Liq. Cryst. **20**, 267 (1973).
[24] M. I. Barnik, L. M. Blinov, M. F. 20, 267 (1973). A.0.333(G.)3rebenkin,272362nd I. R5s386(R5s386(R50/F41Tf1.9999